Properties of prompt muons produced by 28-GeV proton interactions

W. M. Morse, K.-W. Lai, R. C. Larsen, Y. Y. Lee, L. B. Leipuner, and D. I. Lowenstein
Brookhaven National Laboratory, Upton, New York 11973

D. M. Grannan, R. K. Adair, H. Kasha, R. G. Kellogg, M. J. Lauterbach, and M. P. Schmidt
Yale University, New Haven, Connecticut 06520

(Received 12 June 1978)

We have measured prompt dimuon production from the interactions of 28.5-GeV protons with nuclear targets. The dimuon differential cross section $d\sigma/dx$ and the prompt-muon-to-pion ratio are equal within errors to that found at an incident proton beam energy of 400 GeV. The atomic-number dependence is found to be the same as that of the total proton-nucleon cross section. The dimuon invariant-mass distribution is presented.

I. INTRODUCTION

Prompt single-muon and dimuon production have been studied extensively at Fermilab energies.[1] These measurements indicate that prompt muons produced at different energies and angles are unpolarized[2,3,4] and derived largely from the production of pairs[5,6] and that the intensity is roughly 3 times larger than expected from electromagnetic decays of known mesons.[7,8] We present here the results of a prompt-muon experiment performed at 28.5 GeV. We compare the intensity and characteristics of muon production at this energy with that at energies ten times higher. These measurements support the view that a new electromagnetic process which we identify, tentatively, with the parton-annihilation mechanism suggested by Bjorken and Weisberg[9] contributes substantially to lepton pair production.

II. APPARATUS

The diagram of Fig. 1 presents a schematic view of the essentials of the experimental apparatus. Protons from the Brookhaven Alternating-Gradient Synchroton (AGS) were focused onto a target assembly which was designed to allow a wide variety of targets to be placed before the beam; variable-density targets of wolfram (hevi-met), iron, and carbon were used for the single-muon intensity and polarization measurements (the polarization measurements are reported elsewhere[4]), while different solid targets of wolfram, iron, and carbon were used for the muon pair measurements. The target assembly was followed by a 2-m-thick steel hadron absorber and a 60-cm thickness of concrete which helped to attenuate evaporation neutrons produced in the nuclear cascades in the steel. This was followed by six scintillation-counter hodoscopes which are labeled A through F. Each array covered an area 1.8 m by 1.8 m and the arrays were separated by steel absorbers; the counters A through F are separated by 60-cm steel absorbers; hodoscope F is separated from the counter assembly E by a further 2.4 m of steel. The A array consisted of 32 counters arranged to define the path of the muon with a maximum uncertainty of 7 cm at the position of the array for those muons which passed within 50 cm from the center of the array and with a poorer spatial resolution for muons produced at larger angles. The spatial resolution of the downstream hodoscopes was less precise and they were used primarily, to differentiate between the passage of one or two muons through the plane which they defined.

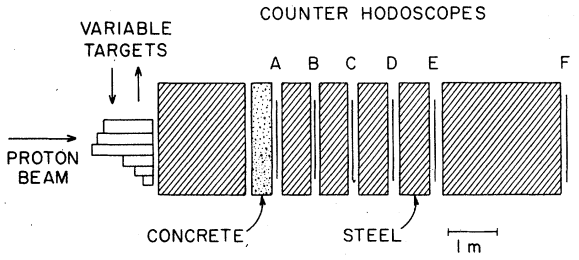

FIG. 1. A schematic diagram of the experimental design.

The different trigger logic used for different aspects of the experimental program set latches for each of the 98 hodoscope counters and these latches were read into a computer memory. After a 200 nsec delay, the latches were read again so that accidental rates could be monitored constantly. While the information from each event and from each machine pulse was written on magnetic tape for possible off-line analysis, most of the results reported here were derived from analyses of data written out in the course of the run.

 © 1978 The American Physical Society

III. MEASUREMENTS OF THE PRODUCTION OF SINGLE MUONS

Measurements of the fluxes of single muons were made using techniques described previously[8] which determine the ratio of single prompt-muons to muons from meson decay in a dense target. Such measurements are especially useful, inasmuch as the measurements define the ratio of muon-pair production to the production of mesons in a manner which is quite insensitive to systematic uncertainties. Here we consider the production of muons produced by the interaction of 28.5 GeV protons with wolfram targets of various densities. A target of solid wolfram (hevi-met) was used as well as targets of wolfram plates separated by air so as to give average densities of $\frac{1}{2}$ and $\frac{1}{3}$ that of the solid target.

The variation of the intensity with respect to target density ρ can be written as

$$I(\rho_1/\rho) = I_p + I_m \times (\rho_1/\rho), \tag{1}$$

where ρ_1 is the density of the solid wolfram; the values of (ρ_1/ρ) are then 1, 2, and 3 for the various measurements. With this parameterization, I_p is the intensity of prompt muons, and I_m is the intensity of muons from the decay of mesons in the solid target. The variation of $d\sigma/dx$ for both meson production and dimuon production with x is very steep, the cross sections decrease sharply with increasing x. As a consequence of the steepness of the spectrum, both I_p and I_m take especially simple forms. In particular, to a good approximation, we can write

$$I_p = 2(d\sigma/dx)_p A_p \, d\Omega_p \quad \text{and} \quad I_m = (d\sigma/dx)_m A_m S_m \, d\Omega_m, \tag{2}$$

where A are longitudinal acceptances equal to $E_{\max}/(E_{\max} - E_{\min})$ for the decay of relativistic mesons and dimuons and $E_{\max}$ and $E_{\min}$ are the maximum and minimum kinematically possible energies from the decay of the parent state in the laboratory system; the acceptances $d\Omega$ represent the effective solid angles subtended by the target, and S_m is the probability of a meson decaying in the target material before interacting and being effectively eliminated from consideration. The value of S_m will be

$$S_m = L/(c\tau E/m), \tag{3}$$

where L is the mean free path for the meson to interact strongly in the target material, m is the meson mass, E the meson energy, and τ the mean life. To a good approximation, the acceptance of the apparatus covers the whole forward production and $d\Omega_m = d\Omega_p$; $A_m \approx 2.5$ while $A_p \approx 1$, except for that small portion of the flux where the invariant mass of the muon pair is very small; the factor of 2 in I_p accounts for the two muons produced by the dimuon decay.

There are corrections in the simple picture outlined above: corrections for the production of muons from secondary mesons and nucleons, corrections and adjustments to account for the contributions of K mesons, as well as pions, to the muon flux, and corrections which take into account the explicit variation of the dimuon flux and the meson flux with x. But these corrections and adjustments are all small, and the adequacy of the very simple picture outlined above produces confidence in the more complete calculations which we use to determine the ratio of $(d\sigma/dx)_m$ and $(d\sigma/dx)_p$. The ratios may then be in error by about 15%, but it is most unlikely that they are grossly in error.

The scaling properties of the single-muon production may be important. If the dimuon differential cross sections obey a limited form of Feynman scaling and $(d\sigma/dx)_p$ is independent of energy, the known scaling of the meson production cross sections requires that

$$(I_p/I_m)_{28\ \mathrm{GeV}} = (I_p/I_m)_{400\ \mathrm{GeV}} \times (28.5/400) \times (184/63.6)^{1/3} \tag{4}$$

for any given value of x where the 400-GeV single-muon intensities were measured using a copper target with $A = 63.6$ and the measurements reported here used wolfram with $A = 184$. The factor (28.5/400) represents the difference in time dilation, and the two factors give the difference in meson survival for the two situations. The graph of Fig. 2 shows the ratios (I_p/I_m) plotted as a function of x for the 28-GeV data and for 400-GeV data[8] taken previously at Fermilab multiplied

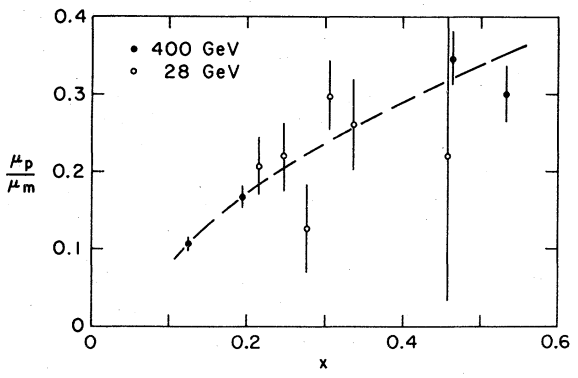

FIG. 2. The ratio of prompt single muons to muons produced in the decay of mesons in the solid target. Dashed curve is drawn to guide the eye.

by the appropriate differential factor. The agreement of the two sets of data shows immediately that the single-muon production scales and then that dimuon production also scales if we accept the evidence which suggests that the single-inclusive-muon flux is derived from muon pair production. We note that systematic uncertainties are minimized by this simple manner of measuring scaling.

IV. MEASUREMENTS OF MUON PAIR PRODUCTION

Measurements of the production of muon pairs were made by requiring signals from two separate muons in the downstream hodoscope counters. Solid targets, 1-mean-free-path thick, of wolfram, iron, and carbon were used. With these targets, muons with energies upon production greater than 2.9 GeV would pass through the A plane while an initial energy of about 9.9 GeV is required for passage through the F plane. The trigger, devised to detect muon pairs produced in the target, required a count in a 1.25-cm × 1.25-cm scintillation counter situated just upstream of the target together with two or more counts from both the A and B hodoscope arrays. About 200 000 protons were accepted per AGS pulse generating about five triggers per pulse.

The triggers were generated both by muon pairs and by hadron showers which penetrate the shielding. In an off-line analysis, both muons were required to penetrate to the C array; 4600 such events were recorded. Assuming all particles reaching the C array are muons the trimuon to dimuon rate is 2%, while the requirement that one muon penetrate to the D array results in a ratio of 0.4%. The above rate of (nominal) trimuons is consistent with rates expected from the hadronic background. Thus the background in the dimuon sample due to hadron showers is negligible.

The intensity of dimuons plotted as a function of Feynman x is shown in Fig. 3. The errors shown are statistical only. The data are well represented over this range of x by the functional forms

$$d\sigma/dx = 40\ \mu\text{b}\ e^{(-10.0 \pm 0.3)x}, \tag{5}$$

$$x d\sigma/dx = 1.8\ \mu\text{b}\,(1-x)^{3.68 \pm 0.09}. \tag{6}$$

Although corrections for muons from the decay of mesons are negligible, there are important modifications of the raw data to account for an acceptance which is a strong function of x. Since we are only sensitive to muons with energies greater than 4.5 GeV, a correction must be made for those muon pairs which decay such that one of the muons does not enter the apparatus. This correction will depend upon the angular distribution of the muons in their own center-of-mass system. These

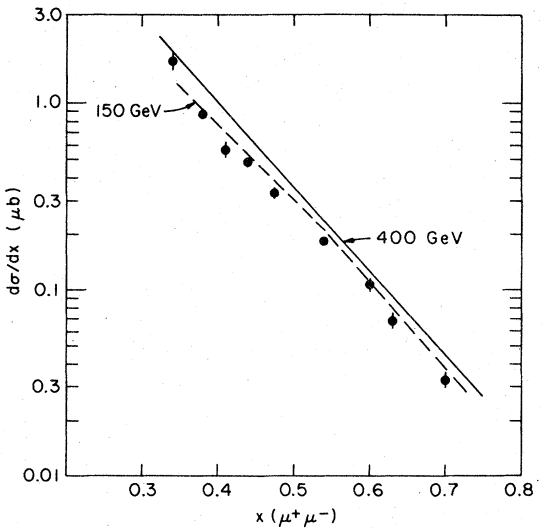

FIG. 3. The intensity of dimuons plotted as a function of x for pairs produced at 28 (solid circles), 150 (dashed curve), and 400 GeV (solid curve).

acceptance corrections were made assuming that the muons are emitted isotropically in their own center-of-mass system. The data did provide a measure of this decay distribution which was consistent with that hypothesis.

We also show on Fig. 3 curves which represent parameterizations of distributions at[7] 150 GeV and at[5] 400 GeV. Although the cross sections appear to increase slightly with energy, the differences of the 28 GeV data reported here and the 400-GeV results with the parameterization of the 150-GeV data are not outside of the systematic uncertainties which accompany these measurements, and we do not consider that the set of results is inconsistent with the Feynman-scaling hypothesis that the differential cross sections $d\sigma/dx$ are independent of energy. This conclusion would be in accord with the analysis of the single-muon data which is subject to different and, we believe, much smaller systematic errors. Dimuon production and hadron production appear to have a similar s dependence over the range of dimuon masses and x studied here. The cross section[10] for the inclusive reaction $pp \to \pi^- + X$ is approximately independent of s for beam energies greater than 28 GeV and $x > 0.20$. Large-mass dimuon production, however, is known to violate Feynman scaling over this energy range.

The graphs of Fig. 4 show the distributions in invariant mass for different ranges of x. Although the mass resolution is poor—the resolution is about 250 MeV/c^2 for a mass of 750 MeV/c^2—this does not much affect the conclusion that the mean invariant mass increases with increasing x. The graph shown in Fig. 5 shows the variation of mean

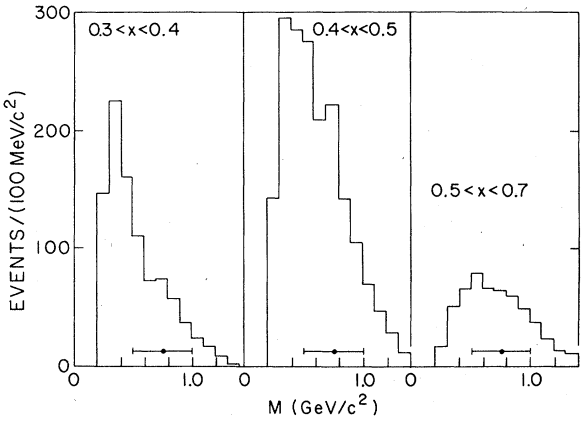

FIG. 4. Dimuon invariant-mass distributions for various ranges of x. The horizontal bar represents the mass resolution.

mass as a function of x for these measurements together with the results given by Chicago-Princeton[7] parameterization of their data taken (with much better resolution) at 150 GeV. The small differences between the two expressions of the data are probably not significant. The result is also in agreement with an early conclusion[5] that, at x near 0.50 at 400 GeV, the mean invariant mass is 900 ± 200 MeV/c^2.

The atomic-number (A) dependence of dimuon production yields information on the production mechanism. The relative dimuon intensity as a function of A is shown in Fig. 6. This experiment measures the A dependence of the production cross section relative to that of the total cross section. We note that the flux is independent of the choice of target indicating an A dependence similar to that of the total cross section. Assuming that the total cross section varies as $A^{2/3}$, we find a dimuon A dependence of $A^{0.64 \pm 0.03}$. This A

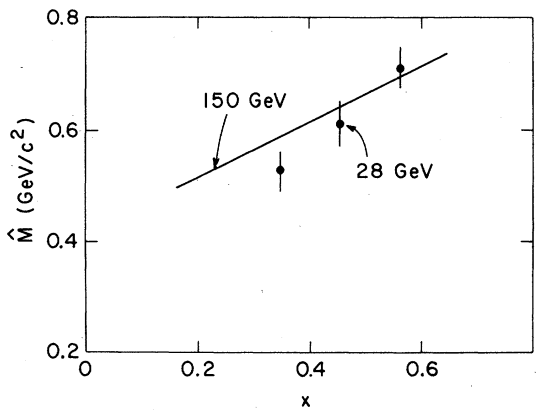

FIG. 5. The mean invariant mass of pairs produced by 28-GeV protons in this experiment. The solid line shows the mean invariant mass taken from data (Ref. 7) at 150 GeV.

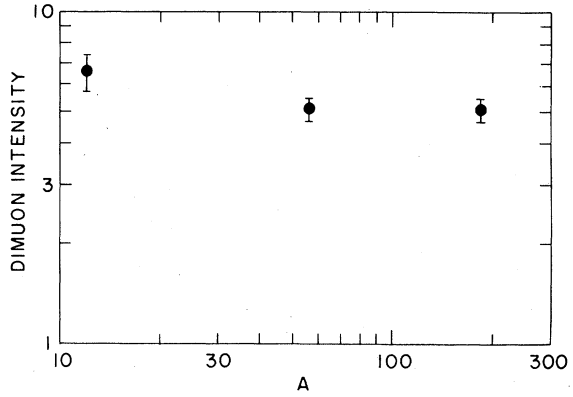

FIG. 6. Dimuon intensity in arbitrary units as a function of the atomic number of the target.

dependence is not a function of dimuon mass or energy over the range we measure. The A dependence so measured is not quite that which might be expected for hadrons. At an x of 0.45 which is about the mean value for the pairs considered here, Eichten *et al.*[11] find a dependence of pion production on A which can be written as $A^{0.54}$. The low-mass dimuon A dependence is also quite different from that of large-mass dimuon production which has an A dependence[12] of approximately A^1.

V. HIGH-RESOLUTION DIMUON MEASUREMENT

In a later run, the apparatus was changed to obtain a high-resolution measurement of the dimuon mass spectrum. The diagram of Fig. 7 presents a schematic view of the essentials of the experimental apparatus. The target consists of five scintillation counters labeled T1 through T5: T1–T4 measure 1.27 cm × 1.27 cm while T5 measures 3.2 cm × 3.2 cm. This was followed by two planes (U and V) of proportional wire chambers with 2-mm wire spacing and two planes (X and Y) of scintillation counters to resolve ambiguities. The active area of the wire chamber measures 25 cm × 26 cm with a dead spot of radius 1.8 cm centered about the beam position. Thus the wire chambers are insensitive to that portion of the

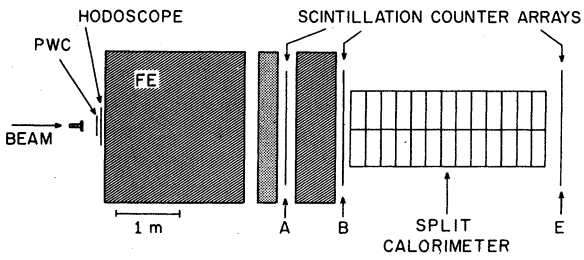

FIG. 7. A schematic diagram of the experimental design.

beam which does not interact in the target. The wire chambers are situated 50 cm downstream of T1.

A split calorimeter is situated downstream of the B plane of scintillation counters. Each arm of the calorimeter consists of thirteen scintillation counters separated by 10-cm steel absorbers. The stopping power of the calorimeter is 2.0 GeV and a muon requires at least 4.0 GeV to reach the calorimeter. Thus only muon pairs with Feynman x between 0.28 and 0.42 stop in the calorimeter. The energy resolution is ± 75 MeV. The trigger for this part of the experiment was devised to detect muon pairs produced in the target. It required a count from T1, an at least twice minimum-ionizing count from T5, two or more counts from the A and B planes, and a muon stop in both sections of the calorimeter: $T1 \cdot T5 (\gtrsim 2) \cdot A(\gtrsim 2) \cdot B(\gtrsim 2) \cdot CAL(2)$. The trajectories of the muons are determined by their reconstructed positions at the proportional wire chambers, and the pulse height information from the five target counters. This trajectory is required to intersect the reconstructed position at the A array within the Coulomb multiple-scattering uncertainty. We require a unique match between the wire-chamber fits and the two A-plane fits. A total of 74 events survive the above criteria.

Possible background to the above sample of dimuon events include pion decay, hadron punch-through, spurious wire-chamber fits, and incorrect muon identification. The first three sources contribute about five events to the above sample. The incorrect-muon-identification source of background has been studied by attempting to fit wire-chamber data to the A-plane data of an unrelated event. This source of background contributes about eight events to the above sample.

Figure 8 shows the dimuon effective mass distribution corrected for the acceptance of the apparatus. We make no subtraction for the small backgrounds discussed above. The mass resolution is about ± 25 MeV/c^2. The significant features of this distribution are a prominent peak at the ρ mass and a broad excess of events the bulk of which lie below the ρ mass. We believe this

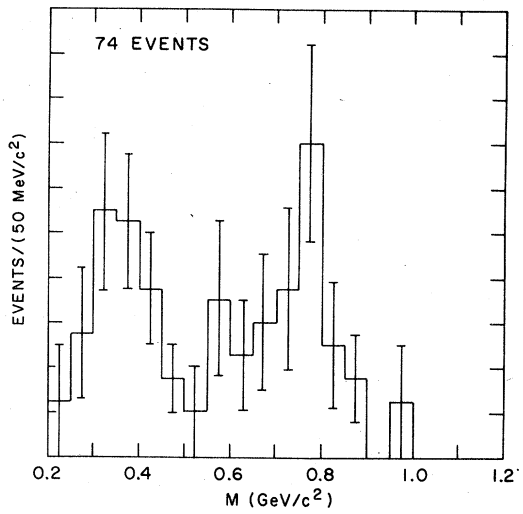

FIG. 8. Dimuon invariant-mass distribution.

dimuon spectrum can be accounted for by ρ, ω, η, and ϕ resonance production and electromagnetic annihilation of parton-antiparton pairs as postulated by Bjorken and Weisberg.[9] We discuss this hypothesis in much more detail in the following article. In as much as the mass distribution shown here is consistent within errors with that of Ref. 7, taken at 150 GeV, we find the differential cross section $d\sigma/dxdm$ to scale with energy.

VI. CONCLUSIONS

In conclusion, we have found a prompt-muon signal for an incident-proton beam momentum of 28.5 GeV. Both the single-muon and dimuon data are consistent with Feynman scaling—that is, the intensity in the fragmentation region is independent of beam energy. The dimuon mass spectrum changes with x both at 28 and 150 GeV—thus each mass region obeys Feynman scaling separately. The A dependence is consistent with a power-law variation $A^{2/3}$ in a x region where pion production varies as $A^{0.54}$.

ACKNOWLEDGMENT

This research was supported in part by the U.S. Department of Energy.

[1]L. M. Lederman, Phys. Rep. 26C, 151 (1976). B. G. Pope, in *High Energy Physics*, proceedings of the European Physical Society International Conference, Palermo, 1975, edited by A. Zichichi (Editrice Compositore, Bologna, 1975); J. H. Christenson *et al.*, Phys. Rev. D 8, 2016 (1973); J. P. Boymond *et al.*, Phys. Rev. Lett. 33, 112 (1974); J. A. Appel, *ibid.* 33, 722 (1974).
[2]L. B. Leipuner *et al.*, Phys. Rev. Lett. 36, 1011 (1975).
[3]M. J. Lauterbach *et al.*, Phys. Rev. Lett. 37, 1436 (1976).
[4]D. M. Grannan *et al.*, Phys. Lett. 69B, 125 (1977).
[5]H. Kasha *et al.*, Phys. Rev. Lett. 36, 1007 (1976).
[6]J. G. Branson *et al.*, Phys. Rev. Lett. 38, 457 (1977).
[7]K. J. Anderson *et al.*, Phys. Rev. Lett. 37, 799 (1976).
[8]L. B. Leipuner *et al.*, Phys. Rev. Lett. 35, 1613 (1975).
[9]J. D. Bjorken and H. Weisberg, Phys. Rev. D 13, 1405 (1976).
[10]W. M. Morse *et al.*, Phys. Rev. D 15, 66 (1977).
[11]T. Eichten *et al.*, Nucl. Phys. B44, 333 (1972).
[12]M. Binkley *et al.*, Phys. Rev. Lett. 37, 571 (1976).